# Spatially modulated 'Mottness' in La$_{2-x}$Ba$_x$CuO$_4$

P. ABBAMONTE[1,2]*, A. RUSYDI[1,3]†, S. SMADICI[1], G. D. GU[1], G. A. SAWATZKY[3,4] AND D. L. FENG[5]

[1]National Synchrotron Light Source and Physics Department, Brookhaven National Laboratory, Upton, New York 11973, USA
[2]Department of Physics, University of Illinois, Urbana, Illinois 61801, USA
[3]Materials Science Centre, University of Groningen, 9747 AG Groningen, The Netherlands
[4]Department of Physics and Astronomy, University of British Columbia, Vancouver, British Columbia V6T-1Z1, Canada
[5]Department of Physics, Fudan University, Shangai 200433, China
†Current address: Institute for Applied Physics, University of Hamburg, D-20355 Hamburg, Germany
*e-mail: abbamonte@mrl.uiuc.edu

**C**ompetition between magnetism and the kinetic energy of mobile carriers (typically holes) in doped antiferromagnets may lead to 'stripe' phases[1–4], which are charged rivers separating regions of oppositely phased antiferromagnetism. In copper oxides the main experimental evidence for such coexisting static spin and charge order comes from neutron scattering in La$_{1.48}$Nd$_{0.4}$Sr$_{0.12}$CuO$_4$ (LNSCO; ref. 5) and La$_{1.875}$Ba$_{0.125}$CuO$_4$ (LBCO; ref. 6). However, as a neutron is neutral, it does not detect charge but rather its associated lattice distortion[7], so it is not known whether the stripes involve ordering of the doped holes. Here we present a study of the charge order in LBCO with resonant soft X-ray scattering (RSXS). We observe giant resonances near the Fermi level as well as near the correlated gap[8,9], demonstrating significant modulation in both the doped-hole density and the 'Mottness', or the degree to which the system resembles a Mott insulator[10]. The peak-to-trough amplitude of the valence modulation is estimated to be 0.063 holes, which suggests[11] an integrated area of 0.59 holes under a single stripe, close to the expected 0.5 for half-filled stripes.

The charge/spin superstructure in LNSCO[5] and LBCO[6] appears only in the low-temperature tetragonal (LTT) phase, is most stable at $x = 1/8$ and coincides with an anomalous suppression of the critical temperature $T_c$ (ref. 12). This phase is frequently interpreted as (quasi) static stripes that have been pinned by the LTT distortion. The charge reflections observed with neutron scattering are weak ($\sim$6 times less intense than the magnetic reflections) as neutrons only detect the lattice distortion, which was estimated to be only about 0.004 Å (ref. 7). However, one assumes that the hole modulation itself is significant. We point out, however, that the spin-density wave in elemental Cr also exhibits half-wavelength charge reflections that are weaker by about a factor of 4.1 and represent a distortion of similar size[13]. So, in the neutron Bragg peaks alone there is no clear difference between the phenomenon in LNSCO and a simple spin-density wave. To determine whether the doped holes are actually involved we have studied LBCO with RSXS near the O K ($1s \rightarrow 2p$) and Cu L$_{3/2}$

($2p_{3/2} \rightarrow 3d_{x2-y2}$) edges, which provide direct sensitivity to valence electron ordering[14–20].

Single crystals of La$_{2-x}$Ba$_x$CuO$_4$ with $x = 1/8$ were grown by the floating-zone method[21]. The sample used in this study had $T_c = 2.5$ K indicating suppressed superconductivity and stabilized spin/charge order. The sample was cleaved in air revealing a surface with $(0, 0, 1)$ orientation. RSXS measurements were performed on beam line X1B at the National Synchrotron Light Source, Brookhaven, using a 10-axis, ultrahigh-vacuum-compatible diffractometer. The sample was cooled with a He flow cryostat connected through Cu braids, providing a base temperature of 18 K. X-ray absorption spectra (XAS) were measured *in situ* in fluorescence yield mode at the O K and Cu L$_{3/2}$ edges and found to be consistent with previous studies[8] (see Figs 1, 3a). We will denote reciprocal space with Miller indices $(H, K, L)$, which represent a momentum transfer $\mathbf{Q} = (2\pi/a \, H, 2\pi/b \, K, 2\pi/c \, L)$ where $a = b = 3.788$ Å, $c = 13.23$ Å. The incident X-ray polarization depends on $\mathbf{Q}$ but was approximately 60° from the Cu–O bond for measurements at both edges.

The O K XAS in the cuprates exhibits a mobile carrier peak (MCP) at 528.6 eV, corresponding to transitions into the doped hole levels, and an upper Hubbard band (UHB) peak at 530.4 eV, corresponding to transitions into the $d$ level of a neighbouring Cu (see Figs 1 and 3). As the hole density increases, spectral weight is transferred from the UHB to the MCP as the number of sites opposing electron addition decreases[8,9,22]. In this letter we take the spectral weight in the MCP to be a measure of the local hole density and that in the UHB to be a measure of the 'Mottness'[10], that is, the degree to which there is a functioning Hubbard $U$, the degree to which the system resembles a Mott insulator. The Cu L$_{3/2}$ edge exhibits a main peak at 933 eV and ligand hole side band at 934.3 eV, which grows with doping. We take the sideband to be a measure of the hole density, similar to the MCP, and the main peak to be a measure of distortions in the Cu sublattice.

Static charge 'stripe' correlations were initially detected at the Cu L$_{3/2}$ resonance and mapped in the $(H, 0, L)$ plane, shown
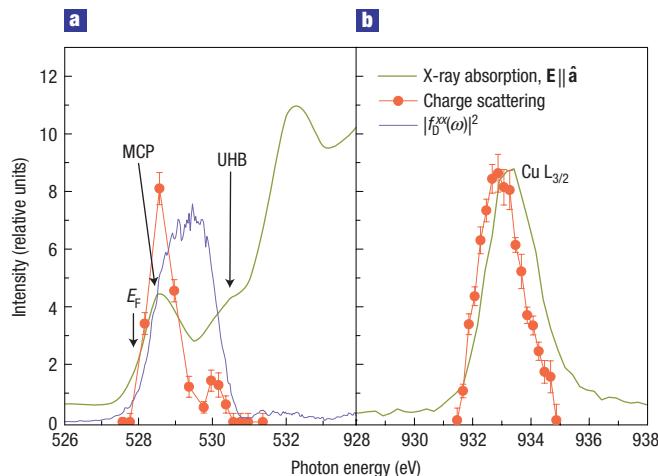
**Figure 1** A 'resonance profile', that is, the energy dependence of the $(1/4, 0, L)$ charge scattering compared with XAS. **a**, Data near the O K edge. Green line, XAS spectrum for $\mathbf{E} \parallel \hat{\mathbf{a}}$ (where $\mathbf{E}$ is the polarization direction and $\hat{\mathbf{a}}$ is the CuO bond direction). Red circles, intensity of charge scattering at $L = 0.72$ showing enhancements at the MCP and UHB, demonstrating a significant modulation of the doped hole density. Blue line, $|f_D^{xx}(\omega)|$ determined in Fig. 3. The energy width of $|f_D^{xx}|$ is larger than the actual data points because the photoelectron lifetime contributes in absorption but not scattering. $E_F$ is the Fermi energy. **b**, Data near the Cu L$_3$ edge for $L = 1.47$. A slight red shift is seen between the peak in resonant scattering compared with absorption. The error bars describe the confidence (interval determined from the chi-squared value and one of the diagonal components of the variance–covariance matrix) in the integrated intensity given statistical noise in the experimental data.



**Figure 2** Reciprocal space map of charge correlations in the $(H, 0, L)$ plane. These data were taken with the X-ray energy tuned to the Cu L$_{3/2}$ $(2p_{3/2} \to 3d_{x2-y2})$ resonance. At its maximum the charge scattering is 175 Hz on a fluorescence background of 450 Hz. As $L$ decreases, the fluorescence intensity rises as the angle of incidence on the crystal grows, reaching its maximum value at $L = 1.38$, below which the takeoff angle falls, driving the intensity to zero through sample self-absorption.

in Fig. 2. In agreement with hard X-ray studies[23,24], the scattering was sharp along $H$ but rod-like along $L$ (correlation lengths $\xi_a \approx 127a$, $\xi_c \approx 2c$), indicating quasi-long-range order in the CuO$_2$ plane but weak coupling between planes. A maximum intensity of 175 Hz on a fluorescence background of 425 Hz was observed at $(0.251, 0, 3/2)$. Owing to differences in beam refraction a slightly different value $H = 0.245$ was observed at the O K edge. The half-integer $L$ indicates that charge order is offset by $2a$ between successive unit cells, presumably to minimize Coulomb repulsion. No scattering could be detected off-resonance above the fluorescence background.

In Fig. 1 we display a 'resonance profile', that is, the intensity of charge scattering as a function of energy compared with XAS. For geometric convenience the O K and Cu L$_{3/2}$ data were taken with $L = 0.72$ and 1.47, respectively. The charge scattering at the Cu L$_{3/2}$ edge is offset from the absorption maximum by 0.2 eV and probably arises from distortions in the Cu sublattice. The O K scattering exhibits strong resonances at both the MCP and UHB features, indicating that the carrier density and the degree of Mottness are both modulated in real space. This shows that this phase exhibits real charge order and, perhaps more significantly, is associated with a periodic restoration of a Mott state.

The charge modulation seems to be substantial but it is important to estimate its size. The integrated intensity of a Bragg reflection is proportional to the square of its structure factor, $\rho_Q^{mn}(\omega) = (1/V_{cell}) \sum_j f_j^{mn}(\omega) \exp(i\mathbf{Q} \cdot \mathbf{r}_j)$, where $V_{cell}$ is the unit cell volume, $f_j^{mn}(\omega)$ is the X-ray form factor of atom $j$, $\mathbf{r}_j$ its position, $\omega$ is the photon energy, and $m$ and $n$ are incoming and outgoing polarization indices[25]. So to estimate the hole amplitude one must first define the X-ray form factor for a doped hole.

For this purpose we separate the oxygen form factor $f_O^{mn}(\omega, p) = f_R(\omega) + p f_D^{mn}(\omega)$, where $f_R$ is a 'raw' component

common to all oxygen atoms, that is, $f_R \to 8$ as $\omega \to \infty$, and $f_D^{mn}(\omega)$ describes the polarization-dependent spectral changes with the doped-hole density, $p$. $f_D^{mn}$ has units of electrons per hole and can be interpreted as the doped hole form factor. A form factor is related to the absorptive part of the index of refraction by $\mathrm{Im}[n^m(\omega; p)] = -r_e \lambda^2 / 2\pi V_{cell} \mathrm{Im}[\sum_i f_i^{mm}(\omega, p)]$, where $r_e$ is the classical electron radius and $\lambda$ is the X-ray wavelength, so $f_D^{mn}$ may be determined from doping-dependent XAS. Using this relationship and data from ref. 8 (Fig. 3a) we extracted the diagonal components $\mathrm{Im}[f_D^{mm}(\omega)]$ by solving a system of equations at each energy and retrieving the real parts by Kramers–Kronig transform. The off-diagonal components were assumed to be small. For an $x$-oriented hole we find $|f_D^{xx}| = 82$ electrons per hole on the resonance maximum, that is, a doped hole scatters as strongly as a Pb atom.

A stripe structure factor $\rho_{stripes}^{mn}$ was constructed based on the orbital pattern from a previous three-band Hubbard calculation[11] to relate $f_D^{mn}(\omega)$ to the scattered intensity (Fig. 3c). This pattern was stacked in alternating fashion as proposed in ref. 7 and, accounting for the incident and scattered polarizations, the structure factor was computed analytically to be $|\boldsymbol{\varepsilon}_f^* \cdot \boldsymbol{\rho}_{stripes} \cdot \boldsymbol{\varepsilon}_i| = A \cdot (0.00475 \, \text{Å}^{-3})$ (where $\boldsymbol{\varepsilon}_i$ and $\boldsymbol{\varepsilon}_f^*$ are the incident and scattered (or 'final') polarizations, respectively). $A$ is a fit variable that may be interpreted as the number of holes contained in one stripe a single unit cell in length ($A = 0.5$ would be consistent with half-filled stripes).

The integrated intensity of resonant scattering was determined in the ellipsoidal approximation by tuning to the MCP and carrying out linear scans along three orthogonal directions, and taking the product $I = I_{peak} \times \Delta q_x \Delta q_y \Delta q_z$, where $I_{peak}$ is the peak count rate in hertz and $\Delta q_n$ is the width along direction $n$. We measured
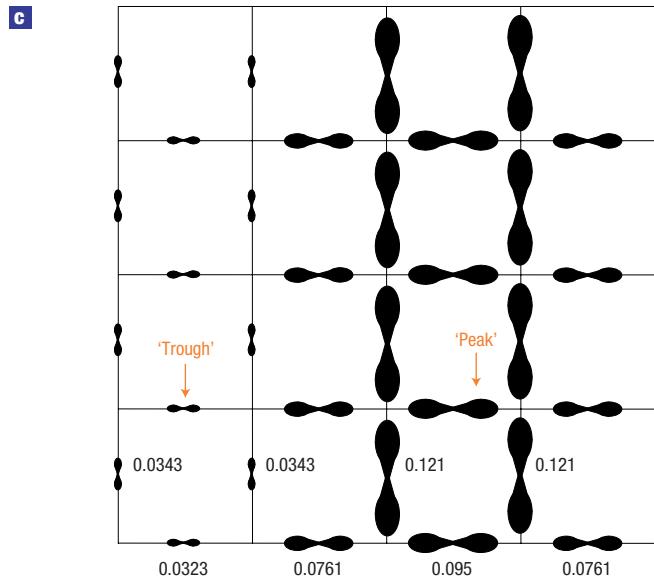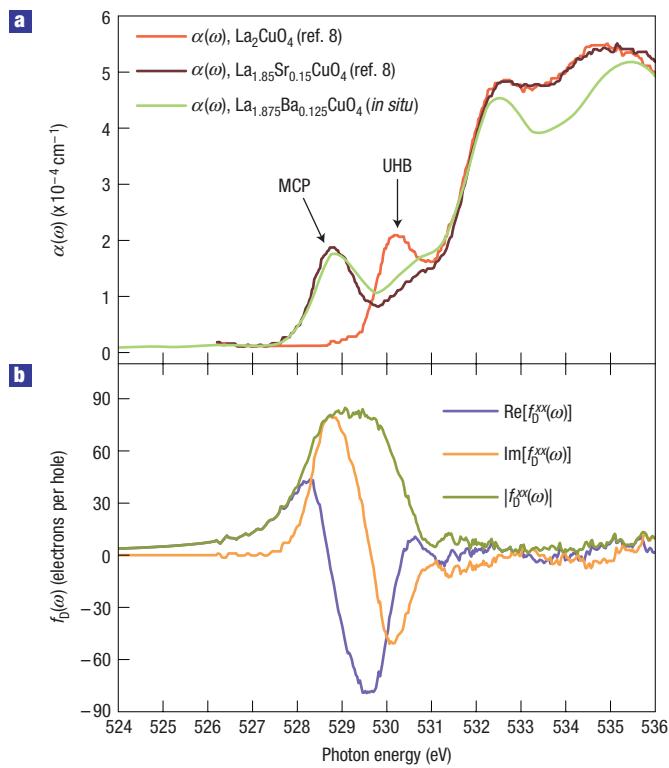
**Figure 3 Determining the X-ray form factor, $f_D^{mn}(\omega)$, for a single doped hole.** **a**, XAS for $La_{2-x}Sr_xCuO_4$ with $x = 0$ (red line) and $x = 0.15$ (black line) for **E** $\parallel$ **â**, reproduced from ref. 8. Spectra were placed on an absolute scale by fitting to tabulated values[28] far from the edge. Data from the current sample (green line) are shown for comparison. **b**, $f_D^{xx}(\omega)$ for an $x$-oriented hole determined by using the expression $Im[n^m(\omega; p)] = -r_e\lambda^2/2\pi V_{cell} Im[\Sigma_i f_i^{mm}(\omega, p)]$ to construct a $2 \times 2$ system of equations, matrix inverting to get $Im[f_D^{xx}(\omega)]$ and Kramers–Kroning transforming. $|f_D^{xx}|$ reaches a maximum value of 82 at $\omega = 528.6$ eV, where a single hole scatters as strongly as a Pb atom. **c**, Stripe orbital pattern derived from the three-band Hubbard calculation in ref. 11 with 'peak' and 'trough' locations indicated. Occupancies consistent with the experiment are shown. Note that despite the large integral the peak-to-trough amplitude is only 0.063 holes, as the doped holes are distributed over many sites.
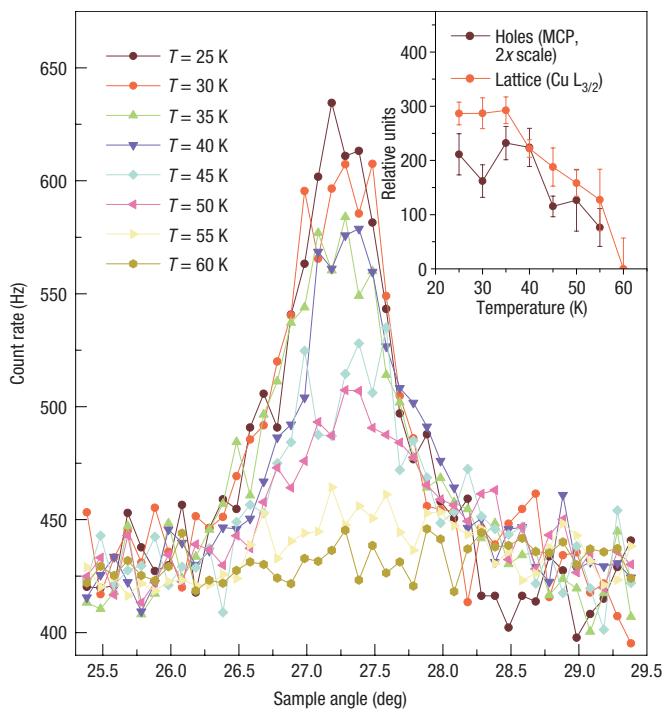
**Figure 4 Temperature dependence of the charge scattering.** Charge correlations are visible below the LTT phase transition temperature $T_{LTT}$ of 60 K. $T_{LTT}$ is higher than previously reported because $x$ is closer to $1/8$. Inset: Charge scattering at both edges exhibits the same temperature dependence, suggesting that the holes and lattice order together. The error bars indicate the square root of the number of counts.

$\Delta q_x = 0.0133$ Å$^{-1}$ and $\Delta q_y = 0.0169$ Å$^{-1}$. The limited **Q** range of RSXS prevented complete determination of $\Delta q_z$ so we use the value from ref. 6 of $\Delta q_z = 0.256$ Å$^{-1}$, giving $I_{stripes} = 0.101$ Hz Å$^{-3}$. To determine the absolute scale, the same measurement was done 10 eV below the O K edge on the $(0, 0, 2)$ Bragg reflection from a cleaved single crystal of $Bi_2Sr_2CaCu_2O_{8+\delta}$, which has a known structure factor. Comparing the two, correcting for differences in absorption, we arrive at $|\varepsilon_f^* \cdot \rho_{stripes} \cdot \varepsilon_i| = 0.00282$ Å$^{-3}$ or $A = 0.59$ holes. This number is only an estimate but is close to the value 0.5 expected for half-filled stripes. The estimated occupancies for various orbitals are shown in Fig. 3c. Note that despite the large integral the peak-to-trough amplitude is only 0.063 holes, as the doped holes are distributed over many sites.

To search for a difference between the ordering of holes and the lattice, angular scans through the charge scattering were performed at different temperatures at both the MCP and Cu $L_{3/2}$ resonances (Fig. 4). Charge correlations were visible at both edges below the LTT transition at 60 K, which is higher than previously published[6] because the $x$ value for our sample is closer to $1/8$ (ref. 26). No difference in temperature dependence was detected between the two edges, suggesting that the holes and lattice order simultaneously.

The reader may wonder about the relationship between this study and the negative result reported in ref. 12 for optimally doped $La_2CuO_{4+y}$ (LCO), in which the stripe order is sometimes said to be 'dynamic'. It is well known that a fluctuating density can give rise to diffuse, elastic scattering, a common example being Rayleigh scattering by the atmosphere. In ref. 14 we showed that the resonant diffuse scattering from such fluctuations in LCO is negligible, that is, such correlations may be valid excited states but

are not thermally occupied, therefore translational symmetry is not broken even on short timescales. By contrast the charge ordering in LBCO is static and, as evident from the large amplitude and the broad spectral width, a macroscopic fraction of the doped holes are modulated. The amplitude of 0.063 is similar to an estimate for Nickelate stripes[20] even though the lattice in LBCO is only weakly involved. The associated modulation of high-energy spectral weight is strong evidence that this phase is driven instead by a desire of the system to restore a Mott state in some regions of the sample.

Our results do not establish whether this phase is truly nematic or is, for example, a 'checkerboard' Wigner crystal[27]. Forthcoming measurements will address this issue. In the meantime, we point out the similarity of this phenomenon to the 'hole crystal' observed in $Sr_{14}Cu_{24}O_{41}$ (ref. 17). The importance of Umklapp processes for the stability of a Wigner crystal on a lattice may explain the stability charge order at the commensurate doping $x = 1/8$.

## References

1. Zaanen, J. & Gunnarsson, O. Charged magnetic domain lines and magnetism of high-$T_c$ oxides. *Phys. Rev. B* **40**, R7391–R7394 (1989).
2. Löw, U., Emery, V. J., Fabricius, K. & Kivelson, S. A. Study of an Ising model with competing long- and short-range interactions. *Phys. Rev. Lett.* **72**, 1918–1921 (1994).
3. Machida, K. Magnetism in $La_2CuO_4$ based compounds. *Physica C* **158**, 192–196 (1989).
4. Poilblanc, D. & Rice, T. M. Charged solitons in the Hartree-Fock approximation to the large-U Hubbard model. *Phys. Rev. B* **39**, 9749–9752 (1989).
5. Tranquada, J. M., Sternlieb, B. J., Axe, J. D., Nakamura, Y. & Uchida, S. Evidence for stripe correlations of spins and holes in copper-oxide superconductors. *Nature* **375**, 561–563 (1995).
6. Fujita, M., Goka, H., Yamada, K. & Matsuda, M. Competition between charge- and spin-density-wave order and superconductivity in $La_{1.875}Ba_{0.125-x}Sr_xCuO_4$. *Phys. Rev. Lett.* **88**, 167008 (2002).
7. Tranquada, J. M. *et al.* Neutron-scattering study of stripe-phase order of holes and spins in $La_{1.48}Nd_{0.4}Sr_{0.12}CuO_4$. *Phys. Rev. B* **54**, 7489–7499 (1996).
8. Chen, C. T. *et al.* Out-of-plane orbital characters of intrinsic and doped holes in $La_{2-x}Sr_xCuO_4$. *Phys. Rev. Lett.* **68**, 2543–2546 (1992).
9. Eskes, H. & Sawatzky, G. A. Doping-dependence of high-energy spectral weights for the high-$T_c$ cuprates. *Phys. Rev. B* **43**, 119–129 (1991).
10. Stanescu, T. D. & Phillips, P. Nonperturbative approach to full Mott behavior. *Phys. Rev. B* **69**, 245104 (2004).
11. Lorenzana, J. & Seibold, G. Metallic mean-field stripes, incommensurability, and chemical potential in cuprates. *Phys. Rev. Lett.* **89**, 136401 (2002).
12. Moodenbaugh, A. R., Xu, Y., Suenaga, M., Folkerts, T. J. & Shelton, R. N. Superconducting properties of $La_{2-x}Ba_xCuO_4$. *Phys. Rev. B* **38**, 4596–4600 (1988).
13. Hill, J. P., Helgesen, G. & Gibbs, D. X-ray-scattering study of charge- and spin-density waves in chromium. *Phys. Rev. B* **51**, 10336 (1995).
14. Abbamonte, P. *et al.* A structural probe of the doped holes in copper-oxide superconductors. *Science* **297**, 581–584 (2002).
15. Wilkins, S. B. *et al.* Direct observation of orbital ordering in $La_{0.5}Sr_{1.5}MnO_4$ using soft x-ray diffraction. *Phys. Rev. Lett.* **91**, 167205 (2003).
16. Thomas, K. J. *et al.* Soft x-ray resonant diffraction study of magnetic and orbital correlations in a manganate near half doping. *Phys. Rev. Lett.* **92**, 237204 (2004).
17. Abbamonte, P. *et al.* Crystallization of charge holes in the spin ladder of $Sr_{14}Cu_{24}O_{41}$. *Nature* **431**, 1078–1081 (2004).
18. Dhesi, S. S. *et al.* Unraveling orbital ordering in $La_{0.5}Sr_{1.5}MnO_4$. *Phys. Rev. Lett.* **92**, 56403 (2004).
19. Freeland, J. W. *et al.* Full bulk spin polarization and intrinsic tunnel barriers at the surface of layered manganates. *Nature Mater.* **4**, 62–67 (2005).
20. Schüßler-Langeheine, C. *et al.* Spectroscopy of stripe order in $La_{1.8}Sr_{1.2}NiO_4$ using resonant soft x-ray diffraction. *Phys. Rev. Lett.* **95**, 156402 (2005).
21. Gu, G. D., Takamuku, K., Koshizuka, N. & Tanaka, S. Large single crystal Bi-2212 along the c-axis prepared by floating zone method. *J. Cryst. Growth* **130**, 325–329 (1993).
22. Eskes, H., Meinders, M. B. J. & Sawatzky, G. A. Anomalous transfer of spectral weight in doped strongly correlated systems. *Phys. Rev. Lett.* **67**, 1035–1038 (1991).
23. Kimura, H. *et al.* Synchrotron x-ray diffraction of a charge stripe order in 1/8-doped $La_{1.875}Ba_{0.125-x}Sr_xCuO_4$. *Phys. Rev. B* **67**, R140504 (2003).
24. von Zimmermann, M. *et al.* Hard-X-ray diffraction study of charge stripe order in $La_{1.48}Nd_{0.4}Sr_{0.12}CuO_4$. *Europhys. Lett.* **41**, 629–634 (1998).
25. Warren, B. E. *X-Ray Diffraction* (Dover, New York, 1990).
26. Axe, J. D. *et al.* Structural phase transitions and superconductivity in $La_{2-x}Ba_xCuO_4$. *Phys. Rev. Lett.* **62**, 2751–2754 (1989).
27. Hanaguri, T. A 'checkerboard' electronic crystal state in lightly hole-doped $Ca_{2-x}Na_xCuO_2Cl_2$. *Nature* **430**, 1001–1005 (2004).
28. Henke, B. L., Gullikson, E. M. & Davis, J. C. X-ray interactions: photoabsorption, scattering, transmission, and reflection at $E = 50$–$30000$ eV, $Z = 1$–92. *At. Data Nucl. Data Tables* **54**, 181–342 (1993).

## Competing financial interests

The authors declare that they have no competing financial interests.